Since January 2020 Elsevier has created a COVID-19 resource centre with free information in English and Mandarin on the novel coronavirus COVID-19. The COVID-19 resource centre is hosted on Elsevier Connect, the company's public news and information website.

Toxicology and Applied Pharmacology 332 (2017) 129–137

Contents lists available at ScienceDirect

Toxicology and Applied Pharmacology

journal homepage: www.elsevier.com/locate/taap

Identification of anti-viral activity of the cardenolides, Na^+/K^+-ATPase inhibitors, against porcine transmissible gastroenteritis virus

Cheng-Wei Yang [a], Hsin-Yu Chang [a], Hsing-Yu Hsu [a], Yue-Zhi Lee [a], Hsun-Shuo Chang [b], Ih-Sheng Chen [b], Shiow-Ju Lee [a,*]

[a] Institute of Biotechnology and Pharmaceutical Research, National Health Research Institutes, Miaoli 35053, Taiwan, ROC
[b] School of Pharmacy, College of Pharmacy, Kaohsiung Medical University, Kaohsiung 807, Taiwan, ROC

ARTICLE INFO

Article history:
Received 15 November 2016
Revised 17 March 2017
Accepted 17 April 2017
Available online 23 April 2017

Keywords:
Cardenolide
Coronavirus
Na^+/K^+-ATPase
Oleandrin
Porcine transmissible gastroenteritis virus
Reevesioside

ABSTRACT

A series of naturally occurring cardenolides that exhibit potent anti-transmissible gastroenteritis virus (TGEV) activity in swine testicular (ST) cells has been identified. In an immunofluorescence assay, these cardenolides were found to diminish the expressions of TGEV nucleocapsid and spike protein, which was used as an indication for viral replication; block TGEV infection induced apoptosis and cytopathic effects; and impart the same trend of inhibitory activity against Na^+/K^+-ATPase as for anti-TGEV activity. The viral titer inhibition was found to take place in a dose-dependent manner. Knocking down expression of Na^+/K^+-ATPase, the cellular receptor of cardenolides, in ST cells was found to significantly impair the susceptibility of ST cells to TGEV infectivity. Thus, we have identified Na^+/K^+-ATPase as an anti-viral drug target and its antagonists, cardenolides, a novel class of anti- TGEV agents.

1. Introduction

Cardenolides, also known as cardiac glycosides, are C(23)-steroids which bind to and act as allosteric inhibitors of Na^+/K^+-ATPase, a membrane-bound protein that establishes and maintains the high internal K^+ and low internal Na^+ cellular concentrations in most animal cells (Agrawal et al., 2012). These Na^+/K^+-ATPases are composed of two subunits (α and β) and an auxiliary subunit γ. The α-subunit binds ATP and both Na^+ and K^+ ions as well as allosteric binding for cardenolides. The combination of α subunit and β subunit have been shown to exhibit different kinetic parameters, including selectivity for cardenolides, and tissue distribution (Baker Bechmann et al., 2016; Habeck et al., 2016; Katz et al., 2015).

Although these naturally occurring cardenolides are often toxic, they have some medical uses. For example, small doses of ouabain, digoxin or digitoxin can be used to treat hypotension, cardiac arrhythmias, or heart failure (Prassas and Diamandis, 2008). Moreover, the use of cardiotonic steroids like ouabain, digitoxin, or oleandrin has been reported as a potential means of combating human cancers (Diederich et al., 2017; Platz et al., 2011); or reducing viral productions of murine leukemia virus, hemagglutinating virus of Japan, and herpes simplex virus type 1 in cultured cells (Nagai et al., 1972; Su et al., 2008; Tomita and Kuwata, 1978). The exact nature and scope of the therapeutic effects of the cardenolides, however, remains to be unraveled.

Coronaviruses (CoV) are glycoprotein-enveloped viruses with a positive-sense single-stranded RNA genome, e.g. human Middle East respiratory syndrome (MERS) CoV, severe acute respiratory syndrome (SARS) CoV, human coronavirus-229E (HCoV-229E), transmissible gastroenteritis coronavirus (TGEV), and murine hepatitis virus (MHV). They are a group of common, ancient, and diverse viruses that cause respiratory, gastrointestinal, and central nervous system diseases; recognize a variety of host receptors, infect many hosts; and are health threats to humans and animals.

The epidemiology for each CoV viral strain is determined by their cognate cell receptor (Chan et al., 2015; Weiss and Navas-Martin, 2005). TGEV belongs to the family Coronaviridae and causes transmissible gastroenteritis, a highly contagious disease which can cause devastating economic losses. TGEV infects all ages and categories of pigs, with mortality rates close to 100% in young pigs. TGEV spike (S) protein binds to the porcine aminopeptidase N, a cell membrane receptor, to aide in its entry into cells (Weiss and Navas-Martin, 2005).

Many small chemical molecules exert anti-coronavirus activity via targeting either viral entry or the intracellular viral life cycle (Tong, 2009a, 2009b). In addition, the small protein griffithsin directly targets and interacts with coronaviral spike glycoprotein to interfere with cell entry, thereby exhibiting an efficient inhibition of viral infectivity for broad spectrum of CoV, including TGEV, SARS CoV, and MERS CoV (Millet et al., 2016; O'Keefe et al., 2010). However, there has no report

* Corresponding author.
E-mail address: slee@nhri.org.tw (S.-J. Lee).

http://dx.doi.org/10.1016/j.taap.2017.04.017
0041-008X/

of coronavirus inhibition via targeting membrane proteins that is non-viral receptor. Herein, we identified a membrane protein, Na^+/K^+-ATPase, as an anti-viral novel target and its antagonists, the cardenolides, as antiviral for TGEV.

2. Materials and methods

2.1. Cells, viruses, immunofluorescent assay (IFA), cytopathic effect and cytotoxicity assays

Swine testicular (ST) epithelial cells (ATCC®CRL-1746™) and the Taiwan field isolated virulent strain of TGEV were grown and propagated; IFA and cytopathic effect and cytotoxicity assays regarding TGEV were also as described (Yang et al., 2010, 2007) with only two modifications: 1) test compounds were pretreated for 1 h; 2) ST cells were infected with TGEV at a multiplicity of infection (MOI) of 7 for IFA, 3.5 for cytopathic effect, and 0.01 MOI for determining virus titers.

The murine astrocytoma cell line DBT and the MHV, JHM strain were maintained as described; IFA and cytopathic effect regarding MHV (0.005 MOI) were also performed as described (Lee et al., 2012).

2.2. Na^+/K^+-ATPase activity assay

Adenosine 5′-triphosphatase (ATPase) from porcine cerebral cortex (Sigma Co.) was reconstituted in 40 mM Tris–HCl (pH 7.8), per the manufacturer's instructions. This enzyme hydrolyzes ATP to ADP and orthophosphate. The hydrolysis is coupled with the exchange of sodium and potassium ions across the plasma membrane (Sigma Co.). For the Na^+/K^+-ATPase activity assay, the reaction mixture (50 μl) contained 0.025 U ATPase, 80 mM NaCl, 20 mM KCl, 40 mM Tris–HCl (pH 7.8), 5 mM EGTA, 3 mM ATP·Mg^{2+} (Sigma Co.), and the tested compounds or vehicle as indicated. Briefly, 35 μl of reaction mixture was incubated with the tested compound (5 μl in DMSO) for 15 min at 37 °C, and then 15 μl of ATP·Mg^{2+} (Sigma Co.) were added at 37 °C to initiate the enzymatic reaction for 30 min. The reaction was quenched by the addition of 3 μl of 30% trichloroacetic acid, and then subjected to centrifugation at 6000 × *g* for 10 min. The resulting supernatant was diluted with H_2O to measure the Pi generated in the enzymatic reaction using the molybdenum blue method (P_iColorLocker™ALS reagent, Innova Biosciences). Further colorimetric development was read at 600 nm using a Beckman Coulter Paradigm™ detection platform.

2.3. Chemicals, western blot analysis, and viral RNA isolation

These assays were performed as described (Yang et al., 2007) using antibodies against GAPDH, β-actin, and caspase-3 (Cell Signaling Technology Inc., MA, USA); and Na^+/K^+-ATPase α1 (Abcam Inc. Cambridge, UK). Tylophorine and Reevesiosides A-I were prepared as described (Chang et al., 2013; Yang et al., 2010). DMSO (D1435, ≧99.5%), digoxin (D6003, ≧95%, HPLC), digitoxin (D5878, ≧92%, HPLC), digitoxigenin (D9404, 99%, TLC), ouabain (O3125, ≧95%, HPLC), dihydroouabain (D0670, ≧98.5%, TLC), oleandrin (O9640, ≧98%, HPLC), N6,2′-O-Dibutyryladenosine 3′,5′-cyclic monophosphate sodium salt (Db cAMP) (D0627, ≧96%, HPLC), and aldosterone (A9477, ≧95%, HPLC) were purchased from Sigma-Aldrich (St. Louis, MO, USA).

2.4. End point dilution assay for determining virus titers

ST cells were plated at a density of 1.8×10^6 cells per well in 6 well-plates containing 1 ml MEM of culture medium (containing 2% FBS), followed by incubation overnight at 37 °C. The tested compounds were added to the wells 1 h prior to the addition of TGEV (0.01 MOI). The plates were then incubated for an additional 22 h at 37 °C as indicated. To quantify the viral yield in the cells, the supernatant of cells in each specific treatment was harvested and subjected to viral titer determination via an end-point dilution assay conducted in ST cells. The mean values and S.D. were calculated from three independent experiments. Serial dilutions of each supernatant were prepared and inoculated to cultured cells in a 96-well plastic plate, which contained an eight sample series of 10-fold dilutions each with 12-repeats. The number of cell cultures that were infected was then determined for each virus dilution, by looking for a cytopathic effect. The endpoint of viral dilution leading to cytopathic effect in 50% of inoculated wells was estimated using the Reed Muench method and designated as one TCID50 (Tissue Culture Infective Dose). TCID50 was then used for the measure of infectious TGEV virus titer as approximately 1 TCID = 0.69 PFU (Plaque-forming unit).

2.5. Na^+/K^+-ATPase gene silence

The pseudotyped lentivirus containing Na^+/K^+-ATPase α1 shRNA (ATP1A1-shRNA) (clone ID: TRCN0000332624 and TRCN0000444902) or negative control-shRNA (shLacZ, clone ID: TRCN231722) (Academia Sinica, Taiwan) were transduced into ST cells with MOI of 3 in culture medium containing 8 μg/ml polybrene (Millipore). At 24 h post transduction, the cells were cultured in the presence of 2 μg/ml puromycin for selection. The selected cells showing knockdown expression of Na^+/K^+-ATPase were validated by western blot analysis prior to TGEV infection for the followed experiments.

2.6. Expression and purification of MHV nucleocapsid (N) protein and generation of the monoclonal antibody against MHV N protein

cDNA of MHV N protein was amplified by PCR with specific primer pairs tagged *Bam*HI and *Eco*RI restriction enzyme sites respectively, 5′-cgcggatccATGTCTTTTGTTCCTGGGCAAG-3′ and 5′-ccggaattcTTACACATTAGAGTCATCTTCTAACCC-3′. The resultant PCR fragment was digested with *Bam*HI and *Eco*RI and then subcloned into pGEX-6p expression vector to generate an expression plasmid pGEX-6p-MHV-N. The construct pGEX-6p-MHV-N was transformed into *Escherichia coli* strain BL21 (DE3) which was to be induced to express glutathione S-transferase (GST) fused N protein by 1 mM IPTG. The subsequent protein expression, purification, and cleavage of N protein from

Table 1
Enzymatic Na^+/K^+-ATPase inhibition and In vitro anti-transmissible gastroenteritis virus (anti-TGEV) activity of cardenolides in swine testis (ST) cells.

Compound	TGEV IC_{50}(nM) ± SD[a]	Na^+/K^+ ATPase IC_{50}(nM) ± SD[a]	ST CC_{50}[a] (μM)
Reevesioside A	164 ± 47	2297 ± 294	>10
Reevesioside B	4448 ± 395	35,642 ± 3232	>50
Reevesioside C	3981 ± 723	24,299 ± 4219	>50
Reevesioside D	27,342 ± 6774	72,269 ± 4589	>50
Reevesioside E	24,047 ± 4448	25,229 ± 3795	>50
Reevesioside F	304 ± 44	1616 ± 220	>10
epi-Reevesioside F	155 ± 39	1018 ± 218	>10
Reevesioside G /*epi*-Reevesioside G	2790 ± 632	10,758 ± 469	>50
Reevesioside H /*epi*-Reevesioside H	22,386 ± 6383	169,093 ± 4798	>50
Reevesioside I /*epi*-Reevesioside I	16,422 ± 3170	127,255 ± 2225	>50
Digoxin	615 ± 120	2727 ± 124	>10
Digitoxin	373 ± 32	6751 ± 931	>10
Digitoxigenin	622 ± 57	1648 ± 90	>10
Oleandrin	166 ± 8	2611 ± 175	>10
Ouabain	147 ± 28	4046 ± 740	>10
Dihydroouabain	3126 ± 842	14,397 ± 842	>50
Tylophorine[b]	311 ± 70	>500,000	>10

[a] The 50% maximal inhibitory concentration (IC_{50}) (nM) values for TGEV replication were determined by immunofluorescent assay at 6 h post-infection (h.p.i.). In parallel, the 50% maximal cytotoxic concentration (CC_{50}) (μM) values for cytotoxicity of each compound in TGEV infected ST cells were also obtained at 6 h.p.i. Shown are means ± S.D. from 3 to 5 independent experiments, each performed in duplicate.

[b] Tylophorine was served as positive control for anti-TGEV activity (Yang et al., 2010).

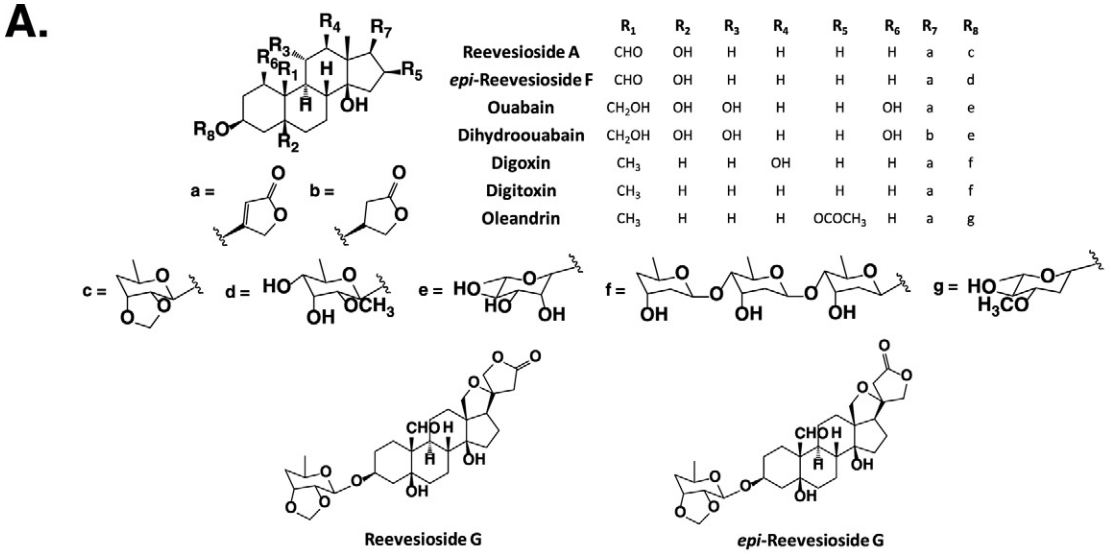

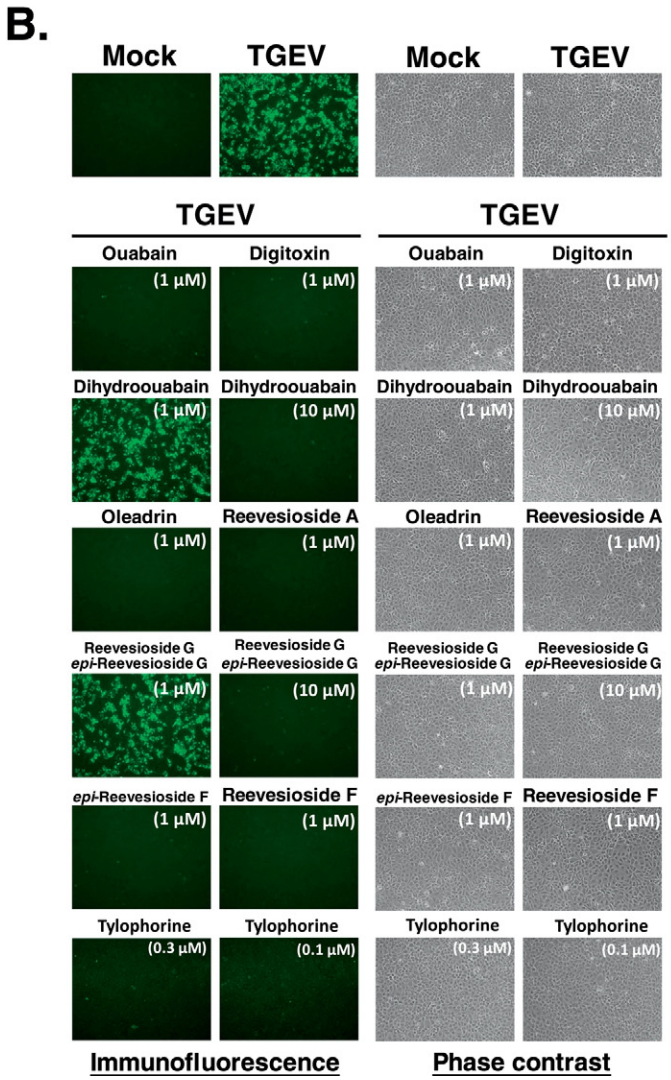

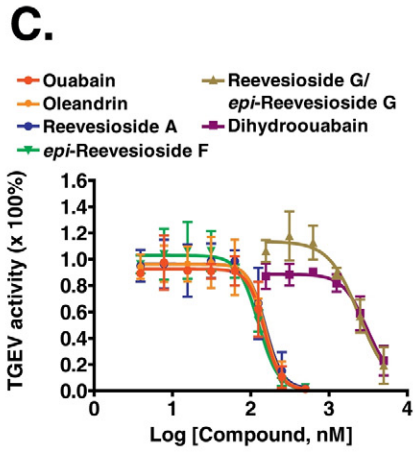

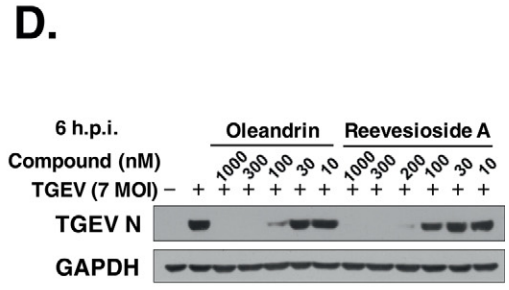

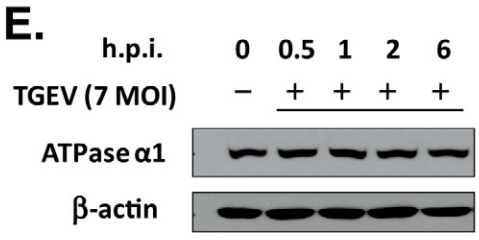

Fig. 1. Chemical structures and anti-TGEV activity of cardenolides. A. Chemical structures of reevesioside A, *epi*-reevesioside F, reevesioside G/*epi*-reevesioside G ouabain, dihydroouabain, and digitoxin. B. Indirect immunofluorescent assay (IFA) with antibodies against S and N protein of TGEV in TGEV (7 MOI) infected ST cells at 6 h.p.i. treated with vehicle (1% DMSO) or cardenolides as indicated. Phase contrast images were shown for the field of ST cells assayed. Shown are representative of three independent experiments. Tylophorine, a phenanthroindolizidine, was used as a positive reference compound for anti-TGEV activities (Lee et al., 2012; Yang et al., 2010). C. TGEV inhibition curves of ouabain, dihydroouabain, oleandrin, reevesioside A, *epi*-reevesioside F, and reevesioside G/*epi*-reevesioside G assayed by IFA. Shown data are average ± S.D. of three independent experiments. The compounds were administered 2 h before viral infection. D. Western analysis for N protein expression in TGEV infected ST cells treated with various doses of oleandrin and reevesioside A. E. Western analysis for Na^+/K^+-ATPase α1 expression in TGEV infected ST cells. Shown are representative of 3 independent experiments.

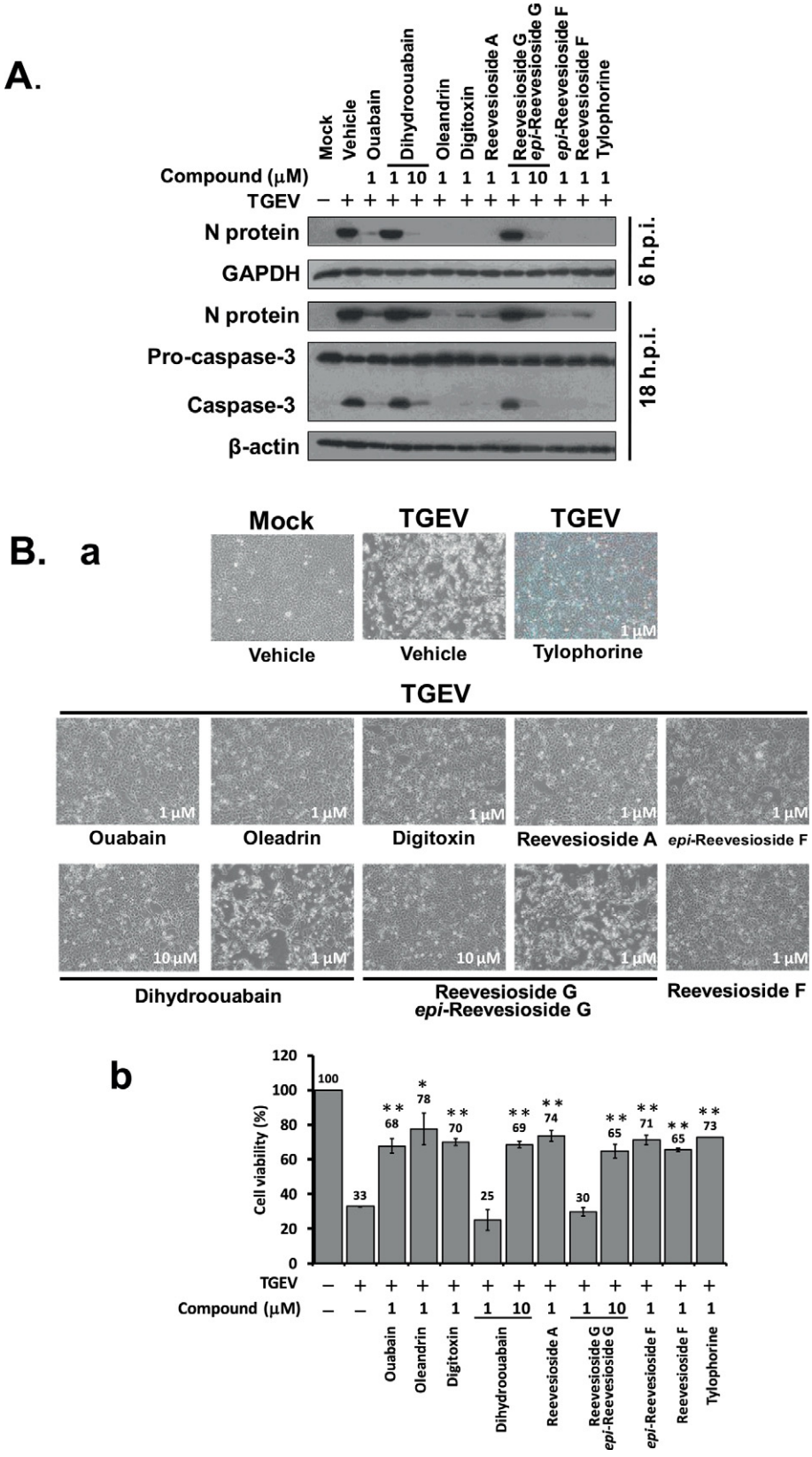

Fig. 2. Effects of cardenolides in TGEV induced caspase-3 activation and cytopathic effect. A. Western blot analysis for cardenolides' effect on caspase-3 activation, N protein production, and β-actin (as an internal loading control) at the indicated concentrations in TGEV infected ST cells at 18 h.p.i. B. Anti-cytopathic effect of cardenolides in TGEV infected ST cells at. Shown are the cytopathic effect of ST cells (a) and cell viability measured by MTS methods (b) with TGEV infection (3.5 MOI) and mock infection at 18 h.p.i. Tylophorine was served as a positive reference compounds for anti-TGEV induced caspase-3 activation and cytopathic effect (Yang et al., 2007). Shown are representative of 3 independent experiments. The survival rates from compound treatments were compared to that of vehicle treatment in TGEV infected ST cells respectively. The Student *t*-test was used to analyzed the significance with *p* values for * <0.05 and ** <0.01.

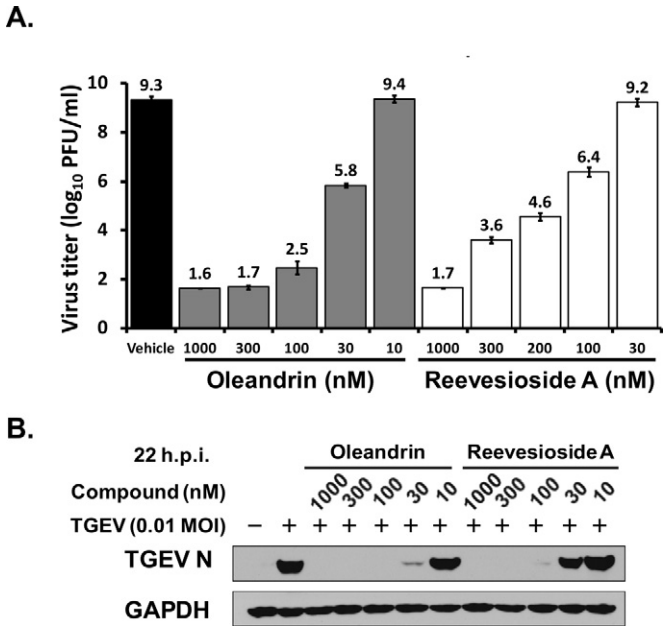

Fig. 3. Effects of cardenolides on reducing TGEV yields. A. Dose dependent effects of reevesioside A and oleandrin on reducing TGEV yields. B. Dose dependent effects of reevesioside A and oleandrin on reducing TGEV N protein expression. ST cells were seeded the day before compound treatment or TGEV infection. The tested compounds were added to the wells 1 h prior to the addition of TGEV (0.01 MOI). The resultant cultures were then incubated for an additional 22 h at 37 °C as indicated. The supernatant of cells in each specific treatment was collected and subjected to viral titers determination via an end-point dilution assay conducted with TGEV infected ST cells, whereas the adherent cells were harvested for western analysis. Results shown were average ± SD or represented results from three more independent experiments.

the GST-MHV N fused protein were carried out as described (Yang et al., 2007).

The purified MHV N protein was used as antigen to generate monoclonal antibody. This work was performed by LTK Laboratories (Taiwan) and carried out according to manufacturer's protocols. Briefly, five mice were immunized each with emulsified 0.02 mg antigen (MHV N protein) in complete adjuvant. After three weeks, five booster injections were given every two weeks with the antigen in incomplete adjuvant. After the fifth injection, the mouse blood was collected for titer testing. Once the mouse was able to produce antibodies against N protein, the mouse's spleen cells were then fused with its myeloma cells to generate immortalized hybridoma cells producing the antibody. Then, the antibody generating hybridoma cells were diluted for obtaining monoclonal hybridoma cells generating monoclonal antibody. The obtained monoclonal hybridoma cell lines, able to generate the antibody reacting with antigen MHV N protein, were individually injected into respective mouse peritoneal cavity and the resultant ascites fluid, containing the monoclonal antibody against MHV N protein, was collected for use in the experiments described.

3. Results

3.1. Identification of cardenolides able to inhibit TGEV replication

A cell-based system comprising TGEV infected ST cells and an IFA (Yang et al., 2007) was used to screen our laboratory collection of natural products from native plants in Taiwan for anti-TGEV agents. The ST cells were pretreated with the test compounds for 1 h prior to infection with TGEV at an MOI of 7. After 6 h of TGEV infection, the ST cells were fixed and subjected to IFA with antibodies specific for the S and N proteins of TGEV. Reevesioside A, reevesioside F, and *epi*-reevesioside F, all possessing structural features similar to those found in the cardenolides, were found to impart potent anti-TGEV activity with IC_{50} values of 164 ± 47 nM, 304 ± 44 nM, and 155 ± 39 nM, respectively. Accordingly, more cardenolides were sought so their anti-TGEV activity could be tested. Digoxin, digitoxin, oleandrin, and ouabain amongst others were also found to impart potent anti-TGEV activities with IC_{50} values of 615 ± 120, 373 ± 32, 166 ± 8, and 147 ± 28 nM, respectively (Table 1). Next, we examined the inhibitory activity of these cardenolides against Na^+/K^+-ATPase and found a correlated trends of inhibition for both TGEV and Na^+/K^+-ATPase (Table 1). The represented structures and dose dependent inhibition curves for IC_{50} values from IFA results of these compounds are shown in Fig. 1A, B and C respectively. Moreover, the N protein expression by western analyses in TGEV infected ST cells also exhibited a dose dependent manner of decreases by treatments with oleandrin or reevesioside A (Fig. 1D). Na^+/K^+-ATPase α1 protein level was not significantly affected upon TGEV infection in ST cells (Fig. 1E). Thus, these cardenolides, Na^+/K^+-ATPase inhibitors, can protect ST cells from TGEV replication.

3.2. Cardenolides protect TGEV infected ST cells from apoptosis and cytopathic effects

TGEV infected ST cells showed significant levels of caspase-3 activation from 14 to 18 h post infection (h.p.i.), as revealed by the cleavage of procaspase-3 to an active caspase-3 (35-kDa to 17- and 19-kDa polypeptides) (Yang et al., 2007). Moreover, TGEV infects ST cells, which subsequently show cytopathic effects such as a rounding and enlargement of cells, formation of syncytia, and detachment of cells into the medium (Yang et al., 2007). At a concentration of 1 μM, ouabain, oleandrin, digitoxin, reevesioside A, reevesioside F, *epi*-reevesioside F, all exerted strong protection against caspase-3 activation; while the less potent dehydroouabain and reevesioside G/*epi*-reevesioside G did not (Fig. 2A). As shown in Fig. 2B, tylophorine, as a positive control, displayed protection against TGEV-infected cytotoxicity and as expected, these cardenolides, at 1 μM, all showed protective effects against cytopathic effect similar to that for anti-caspase-3 activation. Accordingly, the less potent dihydroouabain and reevesioside G/*epi*-reevesioside G at a higher concentration of 10 μM exhibited better protection effects for caspase-3 activation (Fig. 2A) and cytopathic effect than at 1 μM (Fig. 2B). Similar results and conclusion were also obtained by cell viability measured by MTS (Fig. 2C).

3.3. Cardenolides eliminate TGEV titers in a dose dependent manner

Cardenolides reevesioside A and oleandrin were tested for their ability to eliminate TGEV titers. After infection in ST cells, TGEV exhibited a log phase increase in viral yields and reached a plateau from 15 to 22 h.p.i. with titers of ~10^9 p.f.u./ml (data not shown, will be published elsewhere). Treatments with reevesioside A or oleandrin all significantly blocked viral replication and diminished the viral yields, resulting in a reduction of viral yield by ~7 to 8 magnitudes of order at concentrations of 300 nM and 1000 nM (Fig. 3A), and N protein expression (Fig. 3B) in TGEV infected ST cells in a dose dependant manner at 22 h.p.i. These results are consistent with the above described anti-TGEV activities of cardenolides (Figs. 1 & 2, Table 1).

3.4. Depletion of Na^+/K^+-ATPase expression in ST cells decreases the susceptibility of ST cells for TGEV infectivity

Based on above findings, the role of Na^+/K^+-ATPase in anti-TGEV cardenolides was next examined. We knocked down the Na^+/K^+-ATPase α1 expression in ST cells by an RNA silencing approach with two distinct ATP1A1-shRNAs (clone ID: TRCN0000332624 and TRCN0000444902) (see Materials and methods) and obtained the stabling expression clones to test for their response to TGEV infection (Fig. 4). When the Na^+/K^+-ATPase α1 expression was knocked down to 34 ± 13% and 64 ± 3% respectively, the resultant TGEV infected cells expressed relatively less TGEV N protein, 26 ± 6% and 47 ± 9%

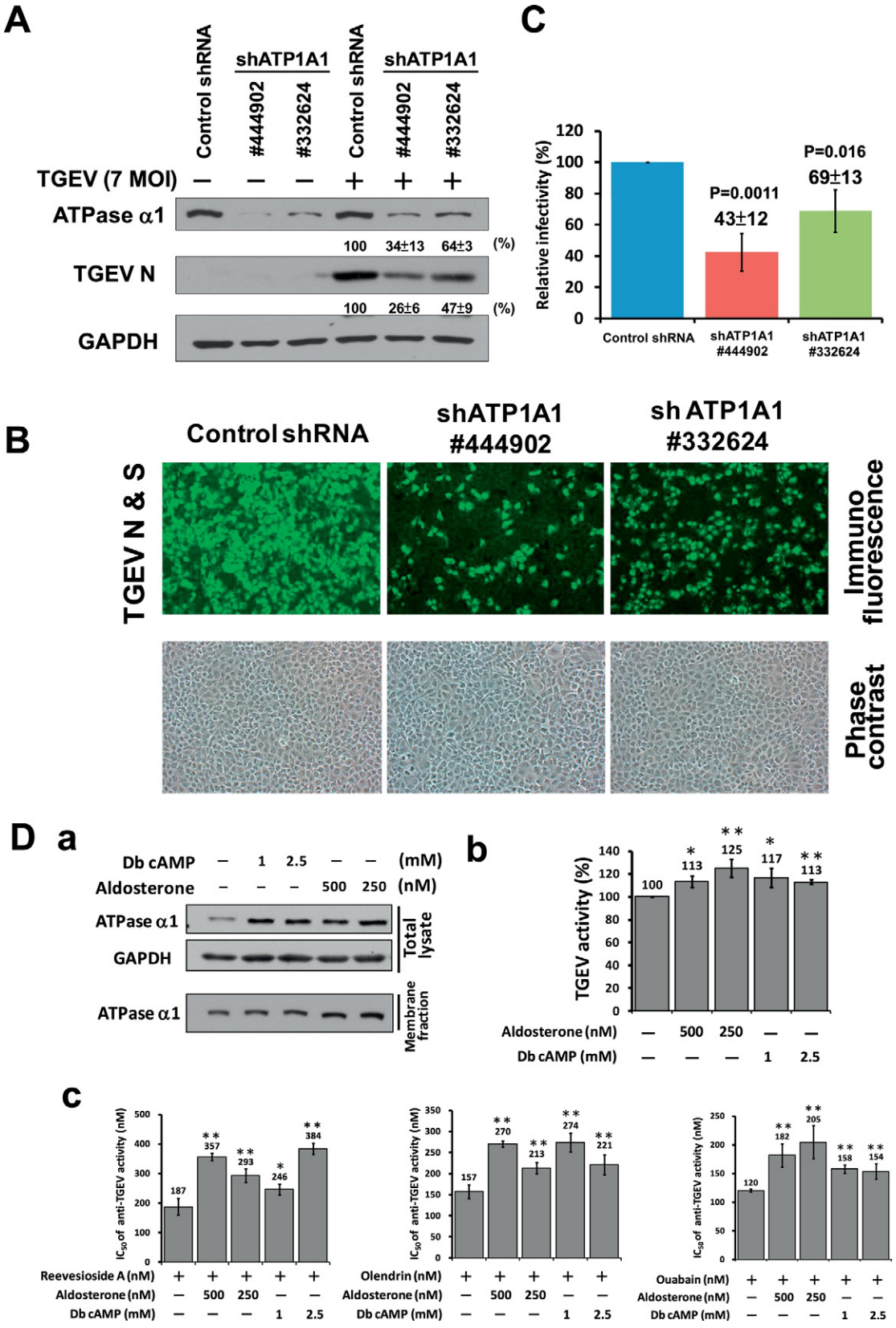

Fig. 4. Depletion of Na^+/K^+-ATPase expression decreased the susceptibility of ST cells to TGEV infectivity. A. Na^+/K^+-ATPase α1 knock-downed ST cells harboring ATP1A1-shRNA expressed significantly less TGEV N protein when infected by TGEV compared to ST cells harbored control-shRNA. The relative expression levels of Na^+/K^+-ATPase α1 and TGEV N protein, averages ± S.D., from three experiments were shown below their respective western blot. B. IFA with antibodies against S and N protein in TGEV (7 MOI) infected ST cells at 6 h.p.i. with control or Na^+/K^+-ATPase α1 shRNA (ATP1A1-shRNA). C. Quantization of immunofluorescence shown in B. D. Effect of Na^+/K^+-ATPase activators, aldosterone and Db cAMP, on the Na^+/K^+-ATPase and TGEV activity in ST cells. Results shown are averages ± S.D. or represented results from three more independent experiments. The IC_{50} values from combined treatments were compared to that of cardenolide treatment alone in TGEV infected ST cells respectively. The Student *t*-test was used to analyzed the significance with *p* values for * <0.05 and ** <0.01.

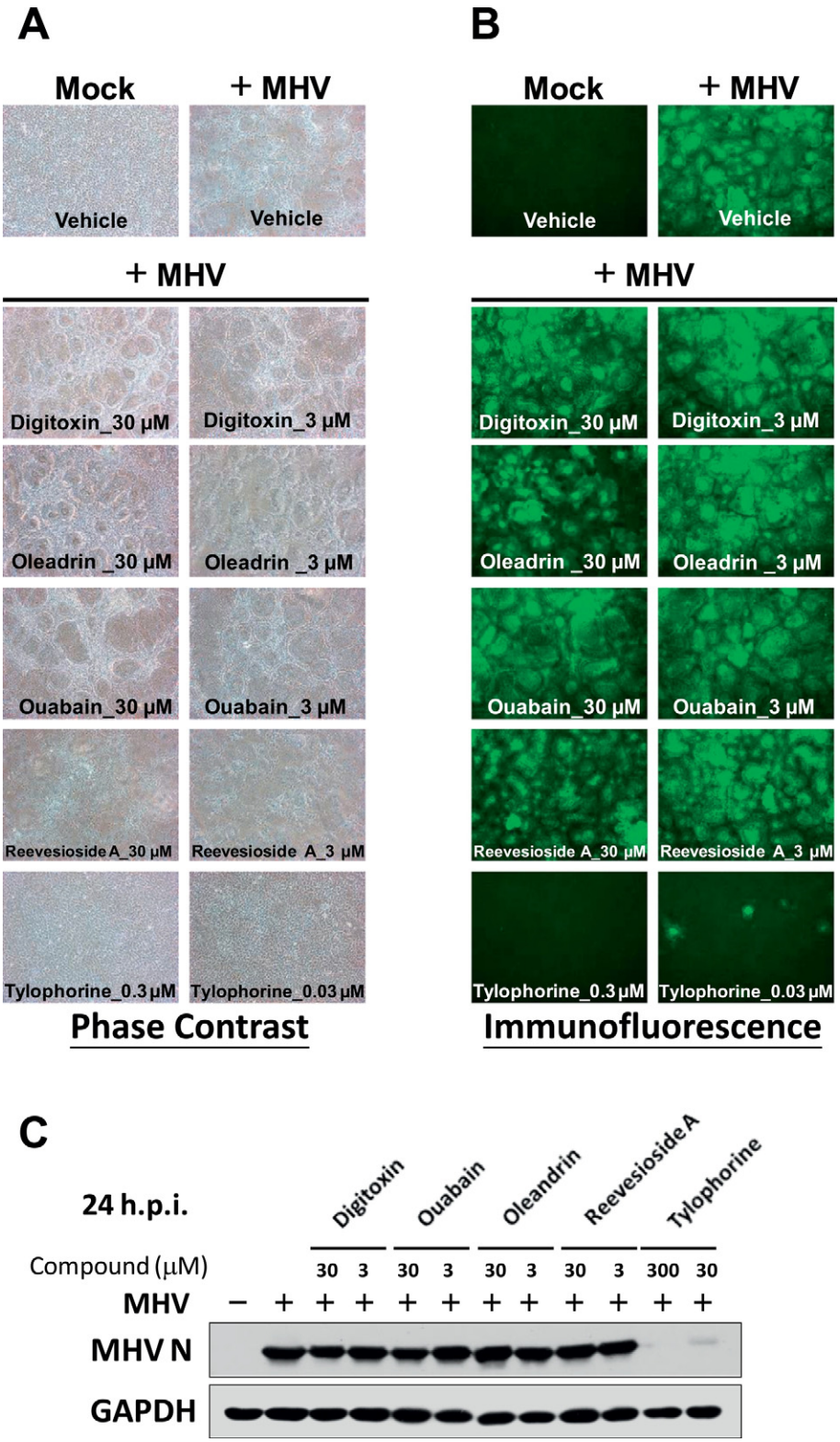

Fig. 5. Cardenolides did not exhibit significant antiviral activities against MHV. A. Cytopathic effects in MHV infected DBT cells with indicated compound treatment. Shown were phase contrast images. B & C. IFA (B) and western analysis (C) for MHV N protein expression in MHV infected DBT cells with indicated compound treatment. The MHV infected cells treated with indicated treatments were fixed at 24 h.p.i. with 80% acetone and subjected to subsequent IFA immunostained with antibody against MHV N protein and phase contrast images were acquired for cytopathic effects. The cell lysates of MHV infected DBT cells with indicated compound treatments at 24 h.p.i. were subjected to western analysis with antibody against MHV N protein. The results shown are representative of three independent experiments.

(Fig. 4A). We then measured the relative TGEV N and S expression level by IFA for TGEV infected cells harboring ATP1A1-shRNAs or control-shRNA and used it as an indication of TGEV infectivity (Fig. 4B). The Na^+/K^+-ATPase depleted cell clones retained 43 ± 12% and 69 ± 13% of infectivity to TGEV respectively, compared to the control-shRNA cells, which correlated the relative Na^+/K^+-ATPase expression levels to the corresponding infectivity (Fig. 4C). Moreover, aldosterone and Db cAMP were reported to increase the Na^+/K^+-ATPase level and

activity (Delamere and King, 1992; Feraille et al., 2003; Gonin et al., 2001; Salyer et al., 2013) therefore we applied them to perform a gain-of-function experiment for Na^+/K^+-ATPase and TGEV infectivity. We found aldosterone and Db cAMP moderately augmented the Na^+/K^+-ATPase protein level in ST cells (Fig. 4D-a) and increased the infectivity of TGEV (Fig. 4D-b). Furthermore, aldosterone and Db cAMP were able to antagonize anti-TGEV activity of cardenolides (Fig. 4D-c). Therefore, we concluded that Na^+/K^+-ATPase contributed to TGEV infectivity in ST cells.

3.5. Cardenolides do not exert anti-MHV activity

The combination of Na^+/K^+-ATPase α and β isoforms determine the selectivity of Na^+/K^+-ATPase inhibition by cardenolides (Baker Bechmann et al., 2016; Habeck et al., 2016; Katz et al., 2015) and host cell receptors differ in coronaviral specific recognition and infection (Millet et al., 2016; Weiss and Navas-Martin, 2005). We then further tested whether cardenolides exert anti-MHV activity. Even at the higher tested concentrations (up to 30 μM) for TGEV, cardenolides did not exhibit any significant protection for MHV infected DBT cells from cytopathic effects (Fig. 5A) induced by MHV nor significantly diminished MHV antigen N protein expression analyzed by IFA (Fig. 5B) and western analysis (Fig. 5C).

4. Conclusion and discussion

Naturally occurring cardenolides such as ouabain, digoxin and digitoxin are often toxic, but can nevertheless be therapeutic for cardiac diseases. Herein, we have explored the antiviral activity of these cardenolides, identified them as a novel class of anti-TGEV agents, and exposed Na^+/K^+-ATPase as a potential drug target for future anti-viral medications.

Different coronaviruses recognize their own specific host cell receptors for infectivity (Blau et al., 2001; Chan et al., 2015; Weiss and Navas-Martin, 2005). The murine coronavirus, MHV, is a coronavirus that causes an epidemic murine illness with high mortality, and infects murine cells through the carcinoembryonic antigen-related cell adhesion molecule-1 (CAE-CAM-1), a cell surface receptor, receptor for attachment and entry (Blau et al., 2001; Weiss and Navas-Martin, 2005). TGEV uses and binds membrane aminopeptidase N as its cell receptor for viral entry (Weiss and Navas-Martin, 2005). The identified anti-TGEV cardenolides did not exert anti-MHV activity in terms of reduction in MHV induced cytopathic effects and viral protein expression (Fig. 5). Moreover, cardenolides inhibit Na^+/K^+-ATPase with selectivity over the combination of its α (α1-α4) and β (β1-β3) isoforms (Baker Bechmann et al., 2016; Habeck et al., 2016; Katz et al., 2015) and cells express different relative levels of α subunit which also determines their responsiveness to cardenolides (Yang et al., 2009). Thus, the combination of Na^+/K^+-ATPase α and β isoforms and the specific cell receptor for each coronavirus are suggested to be important for their selectivity of cardenolides against TGEV over MHV. Moreover, it also merits further exploration of anti-viral activity of cardenolides against other coronaviruses. In addition to above mentioned, whether the Na^+/K^+-ATPase coupled cellular signaling pathways (Newman et al., 2008) upon the binding to cardenolides contribute to their anti-TGEV activities is also under investigation in our laboratory.

Furthermore, aminopeptidase N and Na^+/K^+-ATPase both membrane proteins are reported to locate at membrane raft (Dalskov et al., 2005; Navarrete Santos et al., 2000; Welker et al., 2007). Aminopeptidase N is also known to regulate Na^+/K^+-ATPase activity (Kotlo et al., 2007), and thus they are mutually interactive. It is also possible that the inhibitory activity of cardenolides against TGEV takes place partly through this coupling interaction between aminopeptidase N and Na^+/K^+-ATPase, a finding which merits further investigation.

Transparency document

The Transparency document associated to this article can be found, in the online version.

Acknowledgments

This work was funded by the National Health Research Institutes, Taiwan, R.O.C. and the Ministry of Science and Technology, Taiwan, R.O.C. (grants of NSC 102-2628-B-400-002-MY3, MOST 104-2811-B-400-013, and MOST 105-2325-B-400-005). This work was supported by the National Health Research Institutes, Taiwan, R.O.C. The authors acknowledge Dr. Shaw-Fang Yet for proofreading the manuscript. We also would like to acknowledge the assistance from National RNAi Core Facility, Academia Sinica, Taiwan.

References

Agrawal, A.A., Petschenka, G., Bingham, R.A., Weber, M.G., Rasmann, S., 2012. Toxic cardenolides: chemical ecology and coevolution of specialized plant-herbivore interactions. New Phytol. 194 (1), 28–45.
Baker Bechmann, M., Rotoli, D., Morales, M., Maeso Mdel, C., Garcia Mdel, P., Avila, J., et al., 2016. Na,K-ATPase isozymes in colorectal cancer and liver metastases. Front. Physiol. 7, 9.
Blau, D.M., Turbide, C., Tremblay, M., Olson, M., Letourneau, S., Michaliszyn, E., et al., 2001. Targeted disruption of the Ceacam1 (MHVR) gene leads to reduced susceptibility of mice to mouse hepatitis virus infection. J. Virol. 75 (17), 8173–8186.
Chan, J.F., Lau, S.K., To KK, Cheng, V.C., Woo, P.C., Yuen, K.Y., 2015. Middle East respiratory syndrome coronavirus: another zoonotic betacoronavirus causing SARS-like disease. Clin. Microbiol. Rev. 28 (2), 465–522.
Chang, H.S., Chiang, M.Y., Hsu, H.Y., Yang, C.W., Lin, C.H., Lee, S.J., et al., 2013. Cytotoxic cardenolide glycosides from the root of Reevesia formosana. Phytochemistry 87, 86–95.
Dalskov, S.M., Immerdal, L., Niels-Christiansen, L.L., Hansen, G.H., Schousboe, A., Danielsen, E.M., 2005. Lipid raft localization of GABA A receptor and Na^+, K^+-ATPase in discrete microdomain clusters in rat cerebellar granule cells. Neurochem. Int. 46 (6), 489–499.
Delamere, N.A., King, K.L., 1992. The influence of cyclic AMP upon Na,K-ATPase activity in rabbit ciliary epithelium. Invest. Ophthalmol. Vis. Sci. 33 (2), 430–435.
Diederich, M., Muller, F., Cerella, C., 2017. Cardiac glycosides: from molecular targets to immunogenic cell death. Biochem. Pharmacol. 125, 1–11.
Feraille, E., Mordasini, D., Gonin, S., Deschenes, G., Vinciguerra, M., Doucet, A., et al., 2003. Mechanism of control of Na,K-ATPase in principal cells of the mammalian collecting duct. Ann. N. Y. Acad. Sci. 986, 570–578.
Gonin, S., Deschenes, G., Roger, F., Bens, M., Martin, P.Y., Carpentier, J.L., et al., 2001. Cyclic AMP increases cell surface expression of functional Na,K-ATPase units in mammalian cortical collecting duct principal cells. Mol. Biol. Cell 12 (2), 255–264.
Habeck, M., Tokhtaeva, E., Nadav, Y., Zeev, E.B., Ferris, S.P., Kaufman, R.J., et al., 2016. Selective assembly of Na,K-ATPase α2β2 heterodimers in the heart: distinct functional properties and isoform-selective inhibitors. J. Biol. Chem. 291 (44), 23159–23174.
Katz, A., Tal, D.M., Heller, D., Habeck, M., Ben Zeev, E., Rabah, B., et al., 2015. Digoxin derivatives with selectivity for the alpha2beta3 isoform of Na,K-ATPase potently reduce intraocular pressure. Proc. Natl. Acad. Sci. U. S. A. 112 (44), 13723–13728.
Kotlo, K., Shukla, S., Tawar, U., Skidgel, R.A., Danziger, R.S., 2007. Aminopeptidase N reduces basolateral Na^+-K^+-ATPase in proximal tubule cells. Am. J. Physiol. Renal Physiol. 293 (4), F1047–F1053.
Lee, Y.Z., Yang, C.W., Hsu, H.Y., Qiu, Y.Q., Yeh, T.K., Chang, H.Y., et al., 2012. Synthesis and biological evaluation of tylophorine-derived dibenzoquinolines as orally active agents: exploration of the role of tylophorine E ring on biological activity. J. Med. Chem. 55 (23), 10363–10377.
Millet, J.K., Seron, K., Labitt, R.N., Danneels, A., Palmer, K.E., Whittaker, G.R., et al., 2016. Middle East respiratory syndrome coronavirus infection is inhibited by griffithsin. Antivir. Res. 133, 1–8.
Nagai, Y., Maeno, K., Iinuma, M., Yoshida, T., Matsumoto, T., 1972. Inhibition of virus growth by ouabain: effect of ouabain on the growth of HVJ in chick embryo cells. J. Virol. 9 (2), 234–243.
Navarrete Santos, A., Roentsch, J., Danielsen, E.M., Langner, J., Riemann, D., 2000. Aminopeptidase N/CD13 is associated with raft membrane microdomains in monocytes. Biochem. Biophys. Res. Commun. 269 (1), 143–148.
Newman, R.A., Yang, P., Pawlus, A.D., Block, K.I., 2008. Cardiac glycosides as novel cancer therapeutic agents. Mol. Interv. 8 (1), 36–49.
O'Keefe, B.R., Giomarelli, B., Barnard, D.L., Shenoy, S.R., Chan, P.K., McMahon, J.B., et al., 2010. Broad-spectrum in vitro activity and in vivo efficacy of the antiviral protein griffithsin against emerging viruses of the family Coronaviridae. J. Virol. 84 (5), 2511–2521.
Platz, E.A., Yegnasubramanian, S., Liu, J.O., Chong, C.R., Shim, J.S., Kenfield, S.A., et al., 2011. A novel two-stage, transdisciplinary study identifies digoxin as a possible drug for prostate cancer treatment. Cancer Discov. 1 (1), 68–77.
Prassas, I., Diamandis, E.P., 2008. Novel therapeutic applications of cardiac glycosides. Nat. Rev. Drug Discov. 7 (11), 926–935.

Salyer, S.A., Parks, J., Barati, M.T., Lederer, E.D., Clark, B.J., Klein, J.D., et al., 2013. Aldosterone regulates Na(+), K(+) ATPase activity in human renal proximal tubule cells through mineralocorticoid receptor. Biochim. Biophys. Acta 1833 (10), 2143–2152.

Su, C.T., Hsu, J.T., Hsieh, H.P., Lin, P.H., Chen, T.C., Kao, C.L., et al., 2008. Anti-HSV activity of digitoxin and its possible mechanisms. Antivir. Res. 79 (1), 62–70.

Tomita, Y., Kuwata, T., 1978. Suppression of murine leukaemia virus production by ouabain and interferon in mouse cells. J. Gen. Virol. 38 (2), 223–230.

Tong, T.R., 2009a. Therapies for coronaviruses. Part 2: inhibitors of intracellular life cycle. Expert Opin. Ther. Pat. 19 (4), 415–431.

Tong, T.R., 2009b. Therapies for coronaviruses. Part I of II – viral entry inhibitors. Expert Opin. Ther. Pat. 19 (3), 357–367.

Weiss, S.R., Navas-Martin, S., 2005. Coronavirus pathogenesis and the emerging pathogen severe acute respiratory syndrome coronavirus. Microbiol. Mol. Biol. Rev. 69 (4), 635–664.

Welker, P., Geist, B., Fruhauf, J.H., Salanova, M., Groneberg, D.A., Krause, E., et al., 2007. Role of lipid rafts in membrane delivery of renal epithelial Na^+-K^+-ATPase, thick ascending limb. Am. J. Physiol. Regul. Integr. Comp. Physiol. 292 (3), R1328–R1337.

Yang, C.W., Yang, Y.N., Liang, P.H., Chen, C.M., Chen, W.L., Chang, H.Y., et al., 2007. Novel small-molecule inhibitors of transmissible gastroenteritis virus. Antimicrob. Agents Chemother. 51 (11), 3924–3931.

Yang, P., Menter, D.G., Cartwright, C., Chan, D., Dixon, S., Suraokar, M., et al., 2009. Oleandrin-mediated inhibition of human tumor cell proliferation: importance of Na,K-ATPase alpha subunits as drug targets. Mol. Cancer Ther. 8 (8), 2319–2328.

Yang, C.W., Lee, Y.Z., Kang, I.J., Barnard, D.L., Jan, J.T., Lin, D., et al., 2010. Identification of phenanthroindolizines and phenanthroquinolizidines as novel potent anti-coronaviral agents for porcine enteropathogenic coronavirus transmissible gastroenteritis virus and human severe acute respiratory syndrome coronavirus. Antivir. Res. 88 (2), 160–168.